ISSN 2319 – 2518 www.ijeetc.com
Vol. 1, No. 1, October 2012

Research Paper

THE APPLICATION OF PARTICLE SWARM OPTIMIZATION TO PASSIVE POWER FILTER DESIGN FOR 3PHASE 4-WIRE SYSTEM WITH BALANCE AND UNBALANCE LOAD

B Suresh Kumar[1*] and K Ramesh Reddy[2]

Corresponding Author: **B Suresh Kumar, ✉ bskbus@gmail.com*

This paper proposes an optimal design method for Passive power filters (PPFs) power filters set at high voltage levels to satisfy the requirements of Harmonic filtering and reactive power compensation. Multi objective Optimization models for PPF were constructed. Detuning effects and faults were also considered by constructing Constraints during the optimal process, which improved the reliability and practicability of the designed filters. An effective Strategy was adopted to solve the multi objective optimization Problems for the designs of PPF. Furthermore, the Particle swarm optimization algorithm was developed for searching an optimal solution of planning of filters. An application of the method to an industrial case involving harmonic and reactive Power problems indicated the superiority and practicality of the proposed design methods.

Keywords: PPF, HAPF, THD, PSO

INTRODUCTION

Power systems have to cope with a variety of nonlinear Loads which introduce significant amounts of harmonics. IEEE Standard 519-1992 provides a guideline for the limitation And mitigation of harmonics. Passive power filters (PPFs), Active power filters (APFs), and hybrid active power filters (HAPFs) can all be used to eliminate harmonics. For Medium- and high-voltage systems, PPFs and HAPFs appear to be better choices considering cost where the ratings are of several tens of megavolt–amperes. The design of such PPFs and HAPFs is a complicated nonlinear programming problem. Conventional trial-and-error Methods based on engineering experience are commonly used, but the results are not optimal in most cases.

In recent years, Many studies have appeared involving optimal PPF design. A Method based on the sequential unconstrained minimization Technique has been

1 Department of EEE, CBIT, Gandipet, Hyderabad.
2 Department of EEE, GNITS, Shaikpet, Hyderabad 500008.

used for PPF design because of its simplicity And versatility, but numerical instability can Limit the application of this method. PPF design using simulated Annealing has been reported, but the major drawback is the repeated annealing.

Genetic algorithms (gas) have been widely used in PPF design, but the computing burden and convergence problems are disadvantages of this approach. A design method for PPFs using a hybrid differential evolution Algorithm has also been proposed, but the algorithm is Complex, involving mutation, crossover, migrant, and accelerated Operations. For the optimal design of HAPFs, a method based on gas Has been proposed in order to minimize the rating of APF, but no other optimal design methods appear to have been Suggested.

Many methods treated the optimal design of PPFs and HAPFs as a single objective problem. In fact, filter Design should determine the optimal solution where there are multiple objectives. As these objectives generally conflict with One another, they must be cautiously coordinated to derive a Good compromise solution.

In this optimal multi objective designs for both PPFs and HAPFs using an advanced particle swarm optimization (PSO) algorithm are reported. The objectives and constraints were developed from the viewpoint of practicality and the Filtering characteristics.

For the optimal design of PPFs, the capacity of reactive Power compensation, the original investment cost, and the total Harmonic distortion (THD) were taken as the three objectives. The constraints included individual harmonic distortion, fundamental Reactive power compensation, THD, and parallel and Series resonance with the system. For the optimal design of HAPFs, the capacity of the APF, The reactive power compensation, and the THD were taken as The three objectives; the constraints were as for the PPFs.

The Uncertainties of the filter and system parameters, which will Cause detuning, were also considered as constraints during the optimal design process. A PSO-based algorithm was developed to search for the optimal solution. The numerical results of case Studies comparing the PSO method and the conventional trial and- Error method are reported. From which, the superiority and Availability of the PSO method and the designed filters are certified.

SYSTEM UNDER STUDY

A typical 10-kV 50-Hz system with nonlinear loads, as shown in Figure 1, was studied to determine the optimal design for both PPFs and HAPFs. The nonlinear loads are the medium frequency furnaces commonly found in steel plants with abundant harmonic currents, particularly the fifth and seventh orders, as shown in Table 1. The utility harmonic tolerances given in IEEE Standard 519-1992 and the Chinese National Standard GB/ T14549-93 are listed in Table 1 as percentages of the fundamental current. Table 1 shows that current THD, and the 5th, 23rd, and 25th order harmonic currents exceed the tolerances based on both standards. Filters must therefore be installed to mitigate the harmonics sufficiently to satisfy both standards. Both PPF and HAPF are suitable and economical for harmonic mitigation in such systems. In addition, the harmonic voltages are

Figure 1: Single Diagram of System for Case Studies

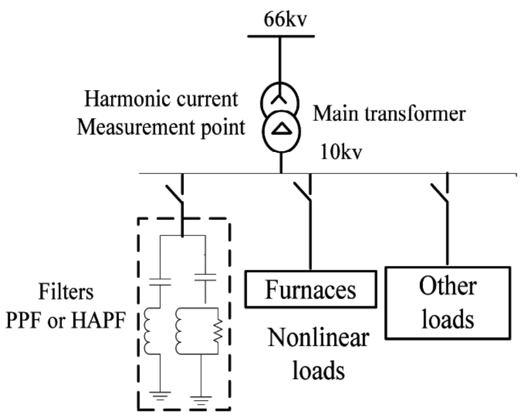

Table 1: Harmonic Current Distributions in Phase A and Utility Tolerances

Harmonic Order	Measured Value (%)	National Standard (%)	IEEE Standard 519-1992 (%)
5	6.14	2.61	4
7	2.77	1.96	4
11	1.54	1.21	2
13	0.8	1.03	2
17	0.6	0.78	1.5
19	0.46	0.7	1.5
23	0.95	0.59	0.6
25	0.93	0.53	0.6
THD	7.12	5	5

in fact very small, so the voltages are assumed to be ideal. The fundamental current and reactive power demands are 1012 A and 3-4 MVar, res-pectively. The short circuit capacity is 132 MVA, and the equivalent source inductance of the system is 2.4 mH.

OPTIMAL DESIGN OF PPFS

A. PPF Structure and Performance

The characteristics of PPFs are detailed in (Mohan *et al*., 1977; Bhattachaya *et al*., 1997; and Yuan et al., 2002). For the system in Figure 1, the approach adopted in this paper utilizes two single-tuned filters and a high-pass damped filter to filter the harmonic currents and to compensate for the reactive power, as shown in Figure 2. The single-tuned filters are used to filter the 5th and 7th order harmonics, while the high-pass damped filter is used to filter the 11th, 23rd, and 25th order harmonics (Yuan et al., 2002).

Figure 2: Single Diagram of System with PPF

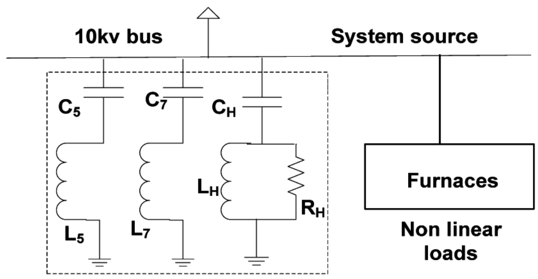

For a single-tuned ûlter, the resonant frequency and quality factor can be expressed using

$$f_i = \frac{1}{2\pi\sqrt{L_i C_i}}, i = 5,7 \qquad \text{...(1)}$$

$$Q = \frac{\omega_i L_i}{R_i} = \frac{1}{\omega_i C_i R_i}, \qquad i = 5,7 \qquad \text{...(2)}$$

where ω_i is the ith angular velocity.

For the high-pass damped filter, the characteristic frequency fH and damping time constant ratio *m* are defined as

$$f_H = \frac{1}{2\pi R_H C_H} \qquad \text{...(3)}$$

$$m = \frac{L_H}{R_H^2 C_H} \qquad ...(4)$$

The equivalent harmonic circuit model of Figure 2 is shown in Figure 3. The nonlinear load is modeled as a harmonic current source, and the system source and PPF are modeled as impedance elements. The other loads will be neglected due to their very large impedance compared with the impedance of system source and the harmonic filter. Thus, the harmonic current Ish through the system source can be expressed as follows (Macken et al., 2001):

Figure 3: Equivalent Harmonic Circuit Model

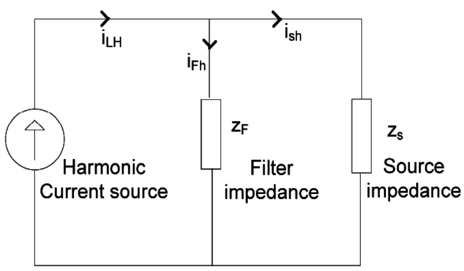

$$I_{sh} = \left|\frac{Z_F}{Z_F + Z_S}\right| I_{Lh} \qquad ...(5)$$

where h is the harmonic order number. I_{Lh} is the h^{th} order harmonic current produced by the nonlinear loads. I_{sh} is the hth order harmonic current to system source. Z_s and Z_F are the equivalent impedances of the system source and the PPF, respectively.

A harmonic attenuation factor γ may be defined as the ratio of *Ish* to *ILh* and defines the filtering performance of a PPF: Better compensation performance can be obtained by decreasing the attenuation factor (Macken et al., 2001). In this case, the attenuation factor is given by

$$\gamma = \frac{I_{sh}}{I_{Lh}} = \left|\frac{Z_F}{Z_F + Z_S}\right| \qquad ...(6)$$

B. Multi objective Optimal Design Model for PPF

The design of PPFs is to determine the types, set number, elements (R, L, and C), and parameters of filters to best satisfy the requirements of harmonic filtering and power factor improvement. In addition, the investment cost of PPF is taken into consideration in the design for constructing the filters with the lowest investment cost. These are formulated in an optimized model with three objectives and some constraints. The constructions of the objectives and constraints are described next.

Three important objectives are constructed as follows.

1. Minimize THD of source current

$$\min THDI = \sqrt{\sum_{h=2}^{N}\left(\frac{I_{sh}}{I_1}\right)^2} \qquad ...(7)$$

where I_1 is the rms value of the fundamental current and N is the highest harmonic order to be considered (in this paper, N = 25).

2. Minimize the initial investment cost

$$\min F = \sum_{i=5,7,H} (K_1 C_i + K_2 L_i + K_3 R_i) \qquad ...(8)$$

where k_1, k_2, and k_3 are cost weighting coefficients with respect to C, L and R [10].

3. Maximize the fundamental reactive power compensation. After installment of the PPF, the power factor of the system should be

close to unity without overcompensation

$$\max \sum_{i=5,7,H} Q_i \quad ...(9)$$

where Q_i is the fundamental reactive power afforded by the i^{th} passive branch.

The constraints are constructed as follows:

It should be noted that the tolerated harmonic levels of the IEEE standard are larger than those of the National standard, so the tolerated levels listed next are based on the National standard. Thus, both the IEEE and National standards are satisfied.

1. Requirements of total harmonic filtering: The THD after compensation must meet the standards

$$THDI \leq THDI_{MAX} \quad ...(10)$$

where $THDI_{MAX}$ is the tolerated level of $THDI$ specified by the National standard.

2. Requirements of individual harmonic filtering: Each order harmonic should satisfy the standard

$$I_{sh} \leq I_{h\max}, h = 5,7,11,13,17,19,23,25 \quad ...(11)$$

where Ih_{max} is the tolerated level of the hth order harmonic current based on the National standard.

3. Fundamental reactive power compensation limits: The fundamental reactive power of filters must be restricted

$$Q_{\min} \leq \sum_{i=5,7,H} Q_i \leq Q_{\max} \quad ...(12)$$

where Q_{min} and Q_{max} are the lower and upper limits of the total fundamental reactive power, respectively.

4. Parallel and series resonance restrictions: To avoid resonance with the system impedance, each filter is constrained to be inductive to the corresponding harmonics to be filtered In addition, the following inequality constraints are added to avoid resonance:

$$\text{Im}(Y_{sh} \| Y_{5h} \| Y_{7h} \| Y_{Hh}) \neq 0 \quad ...(13)$$

$$\text{Im}(Z_{sh} + Z_{5h} \| Z_{7h} \| Z_{Hh}) \neq 0 \quad ...(14)$$

$$h = 5,7,11,13,17,19,23,25$$

where Im(.) is to calculate the imaginary part of a variable. Ysh, $Y5h$, $Y7h$, and YHh are the hth order harmonic admittances of the source system, the 5[th] single-tuned filter, 7[th] single-tuned filter, and high-pass damped filter, respectively. Zsh, $Z5h$, $Z7h$, and ZHh are the hth order harmonic impedances of the source system, the 5[th] single-tuned filter, 7th single-tuned filter, and high-pass damped filter, respectively.

When a filter branch has a fault, only this faulty branch is cut off, and the other branches should work normally (providing the ratings of the unaffected branches are not exceeded). For example, when considering an outage of the fifth single-tuned filter branch, the constraints are constructed as follows:

$$\text{Im}(Y_{sh} \| Y_{7h} \| Y_{Hh}) \neq 0 \quad ...(15)$$

$$\text{Im}(Z_{sh} + Z_{7h} \| Z_{Hh}) \neq 0 \quad ...(16)$$

Other cases with faults are dealt with in similar manner.

C. PSO Method

Recently, Kennedy and Eberhart developed a PSO algorithm based on the behavior of individuals (i.e., particles or agents) of a swarm

(Nakajima et al., 1988). An individual in a swarm approaches to the optimum or quasi-optimum through its present velocity, previous experience, and the experience of its neighbors. Thus, the particle swarm can be used to solve complicated optimization problems in power systems. In a physical *N*-dimensional search space, the position and velocity of the individual *i* are represented as the vectors X_i = (*xi*1*, xi*2*, ..., xiN*) T and *Vi* = (*vi*1*, vi*2*, ..., viN*) T, respectively. Let *Pbesti* = (*xPbesti*1*, xPbesti*2*, ..., xPbestiN*) and *Gbest* = (*xGbest*1 *, xGbest*2 *, ..., xGbestN*) be the best position of an individual *i* and its neighbors' best position so far, respectively. By using this information, the updated velocity and position of individual *i* at iteration *k* are modified using

$$V_i^{k+1} = \omega.V_i^k + c_1.rand_1()*(Pbest_i^k - X_i^k)$$
$$+c_2.rand_2()*(Gbest^k - X_i^k) \quad ...(17)$$

$$X_i^{k+1} = X_i^k + V_i^{k+1}, \qquad i = 1, 2, ..., M \quad ...(18)$$

where *M* is the quantity of particles, *c*1 and *c*2 are weight parameters, *w* is the inertia weight, and *rand*1() and *rand*2() are random numbers between zero and one.

The maximum allowed velocity *V*max determines the searching granularity of space. *X*max is the maximum allowed value for particle position. Generally, the relationship is set as follows:

$$V_{max} = k.X_{max},\ 0.1 \le k \le 0.2 \quad ...(19)$$

Weight parameters *c*1 and *c*2 are scaling factors that determine the relative "pull" of *Pbest* and *Gbest*. These are sometimes referred to as the cognitive and social rates, respectively. The best suggested values for *c*1 and *c*2 are 2.0 [17]. The inertia weight *w* resolves the tradeoff between the global and local exploration abilities of the swarm. A large inertia weight encourages global exploration, while a small one promotes local exploitation. Obviously, varying *w* is suggested to obtain the best performance. In this paper, a linearly decreasing inertia weight with increasing iteration is adopted, as indicated

$$\omega = \omega_{\max} - \frac{\omega_{\max} - \omega_{\min}}{iter_{\max}} * iter \quad ...(20)$$

where $\omega_{\max}$ and $\omega_{\min}$ are the initial and final values of *w*, respectively. $iter_{\max}$ and *iter* are the maximum and current iteration numbers, respectively.

D. Optimal Design for PPF Based on PSO

In this paper, the capacitance of each branch of PPF and the characteristic frequency of the high-pass damped filter are chosen as optimal variables *Xi* = (*C*5*, C*7*, CH, fH*)T, while the tuning frequencies of the fifth and seventh single-tuned filters are predetermined as 242 and 342 Hz, respectively. According to the optimization objectives in,the corresponding fitness functions are as shown as

$$F_1(X) = THDI \quad ...(21)$$

$$F_2(X) = F \quad ...(22)$$

$$F_3(X) = \sum_{i=5,7,H} Q_i \quad ...(23)$$

Then, the optimal design of PPF is obviously a multi objective optimization problem. The usually adopted method for multiobjective optimization is to construct a combinatorial fitness function by integrating all the objectives with linear weights [13], so that the multiobjective optimization problem can be turned into a single objective optimization problem, which is much easier to deal with. However, the combinatorial fitness function has many extreme points, which tends to cause the optimal algorithm to fall into local minimums. This method will also cause unbalance between the different objectives.

In order to overcome these disadvantages, an effective approach is adopted to solve this multiobjective problems i.e from the Equations (21) to (23), Among the three objectives, the most important objective, i.e., *THDI*, is chosen as the final optimization objective, and the other two objectives are considered as "acceptable-level" constraints. These constraints are different from the common constraints referred from the Equations (10)-(16).

$$\min F_1 \quad ...(24)$$

$$F_2 \leq \alpha_1 \quad ...(25)$$

$$\alpha_2 \leq F_3 \leq \alpha_3 \quad ...(26)$$

where α_1, α_3, and α_2 are the highest and lowest acceptable levels for the secondary objectives, respectively.

The overall flowchart for the PPF design based on PSO is shown in Fig. 4 and was implemented using the popular software MATLAB/M file.

Step 1: Initialize a group of particles while satisfying the constraints, including current THD, individual harmonics, fundamental reactive power compensation, and parallel and series resonance with system. Then, calculate the fitness of the initial particles.

Step 2: Update velocity and position of particles.

Step 3: Calculate the new fitness of the updated particles.

Step 4: Check whether the updated particles still satisfy the common constraints, including current THD, individual harmonics, fundamental reactive power compensation, parallel and series resonance with system, and the detuning effect constraints. If not go to Step 7).

Step 5: Check whether the updated particles satisfy the acceptable-level constraints. If not, go to Step 7.

Step 6: Update the *Pbest* and *Gbest*.

Step 7: Check whether the terminal criteria are satisfied. The terminal criteria can be defined as satisfying fitness value or maximum iteration steps. If not, go to Step 2.

The design results of filters using the PSO method and the conventional trial-and-error method are listed in Table 4. The comparisons between the filtering performances of PPFs designed using the PSO method and using the conventional method are shown in Table 5. In addition, the data are simulating results

Figure 4: Flowchart of PPF Optimal Design Based on PSO

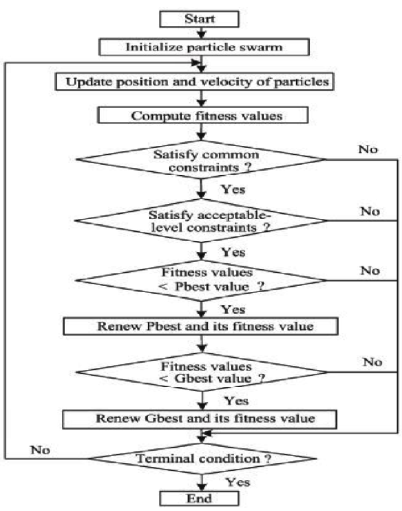

Table 2: Some Parameters Relating to PPF Design

K_1	K_2	K_3	Q_{min}	Q_{max}	α_1	α_2	α_3
2(pu/uf)	3(pu/mH)	5(pu/Ω)	3MVar	4MVar	0.95pu	3.7MVar	4MVar

Table 3: Some Parameters Relating to PSO Algorithm

C1	C2	M	N	$Iter_{max}$	W_{max}	W_{min}
2.0	2.0	20	4	1000	0.9	0.4

Table 4: Design Results of PPFs Based on PSO and Conventional Methods

Design Parameters	PSO-Method	Conventional Method
The 5th Single-tuned filter	C_5=65.48μF L_5=6.1mHQ_5=60	C_5=80.6μ FL_5=5.37mHQ_5=60
The 7th single -tuned filter	C_7=16.54μF L_7=13.09mHQ_7=60	C_7=23.76μF L_7=9.11mHQ_7=60
High-pass damped filter	C_H=41.98μ FL_H=2.12mHm=0.5	C_H=15.28μF L_H=3.32mHm=0.5

Table 5: Harmonic Current Distributions With PPFs Based on PSO and Conventional Methods

Harmonic Orders	PSO Method (%)	Conventional Method (%)
5	1.01	0.82
7	058	0.39
11	0.82	1.13
13	0.32	0.6
17	0.2	0.29
19	0.15	0.21
23	0.3	0.4
25	0.29	0.38
THD	1.54	1.71
Reactive PowerCompensation	4MVar	3.88MVar
cost	0.917pu	1.0pu

based on field measurement data and the same as those in Tables 6, 8-10. It will be seen that all harmonic components and THD of currents fall within the tolerated levels listed in TableI. However, the filtering performance of the PPF designed using the PSO method is significantly better than that designed using the conventional method: The THD is lower (1.54%), the reactive power compensation is greater (4 MVar) and the investment cost is less (saving 8.3% compared with the conventional method), as shown in Table 5. Figure 5 shows the harmonic attenuation factors of PPFs based on the PSO method and on the conventional method and clearly shows the better harmonic attenuation

Table 6: Harmonic Current Distributions With PPF Considering Detuning Effects

Harmonic Orders	PSO Method (%)	Conventional Method (%)
5	2.44	2.0
7	1.36	0.91
11	0.87	1.26
13	0.36	0.62
17	0.24	0.32
19	0.18	0.23
23	0.36	0.46
25	0.35	0.44
THD	3.01	2.77

Figure 5: Harmonic attenuation factors of PPFs (a) Harmonic attenuation factor of PPF based on the PSO method; (b) Harmonic attenuation factor of PPF based on conventional method

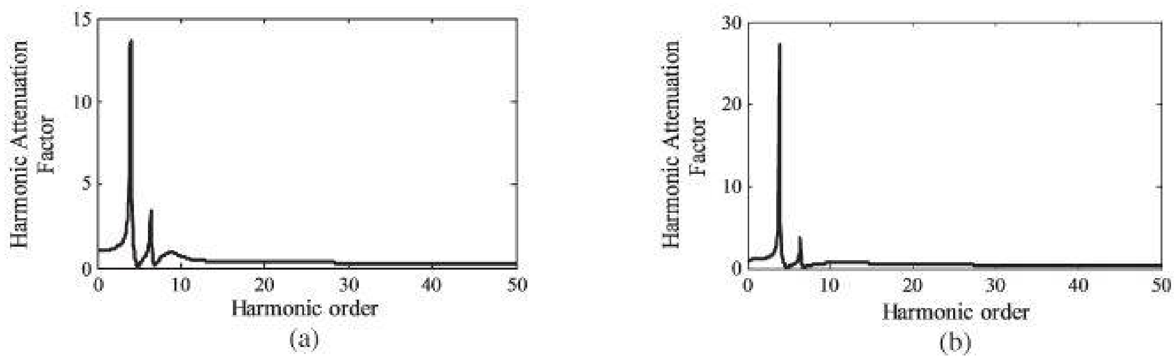

performance of the PPF designed using the PSO method when compared with that designed using the conventional method.

The harmonic attenuation factor defined in this paper has the same meaning as the normalized resultant impedance magnitude seen from harmonic source based on system impedance magnitude (Malesani *et al.*, 1997). Figure 5 also shows that no other resonant point is found. Moreover, there are no harmonic currents at the critical point (the frequency with the largest resultant impedance), and the harmonic currents near the critical point are under control. Hence, it is impossible for the system studied to have resonance when filters are on line under normal conditions.

Table 6 shows the filtering performance under the worst detuning conditions, as described earlier. In the case of the PPF designed using the method based on PSO, the current THD (3.01%) and each order harmonic current are still within the tolerated levels. However, with the conventional method, although the current THD (2.71%) is within the criteria and lower than that using the method based on PSO, the 11th order harmonic current exceeds the tolerated levels of the National standard.

Figure 6: Harmonic Attenuation Factor of the PPF Based on the PSO Method With Detuning Effects

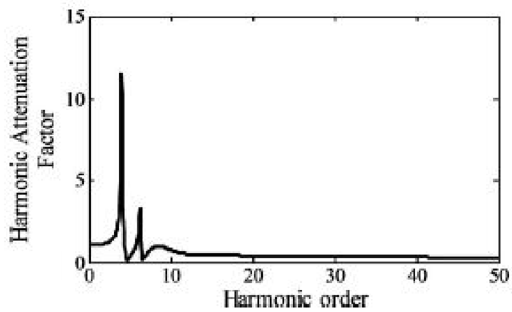

Figure 7: Original Source Current and Its THD Analysis Without PPF (a) Original Source Current of Phase A Without PPF; (b) Thd Analysis of the Original Source Current

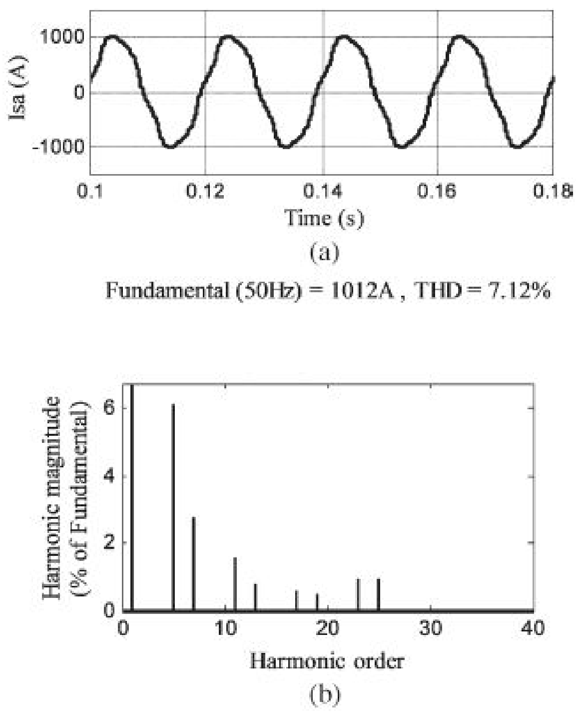

Figure 6 shows the harmonic attenuation factor of the PPF designed using the method based on PSO and considering the worst detuning effects, which is in accordance with the results in Table 6, and no resonance points are found.

Based on field measurement data, some simulation tests were conducted using MATLAB/Simulink. The simulation results are shown in Figures 7 and 8. Figure 7 shows that the original source current is distorted with abundant harmonics, and the current THD is 7.12%. With a PPF designed using the method based on PSO, Figure 8 shows that the compensated source current is close to a pure sine wave, with the current THD decreased to 1.53%.

From the Figure 10 shows the Simulink model of PPF using with and without PSO with Balanced, Unbalanced loads, and the Figure from 10-14 gives the waveforms for load current, source current and filter current ppf conventional and PSO method.

Figure 8: Compensated source current and its THD analysis with PPF designed using the method based on PSO; (a) Compensated source current of phase A with PPF; (b) THD analysis of the compensated source current

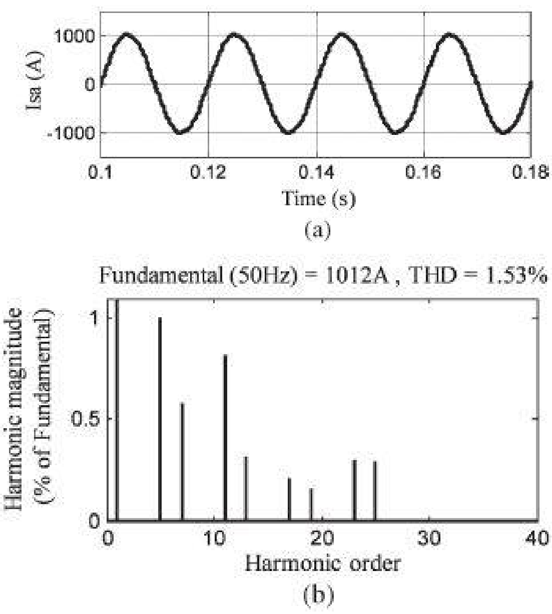

Figure 9: Convergence Characteristics of PSO For Ppf Design

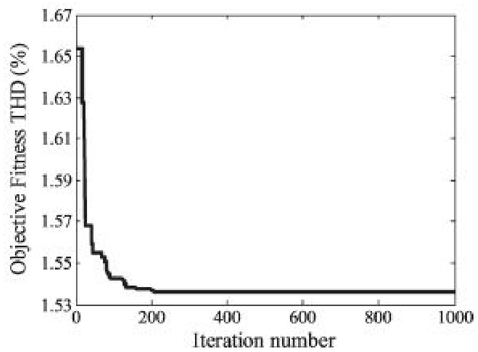

Figure 10: Simulink Model of PPF Using With and Without PSO With Balanced, Unbalanced Loads

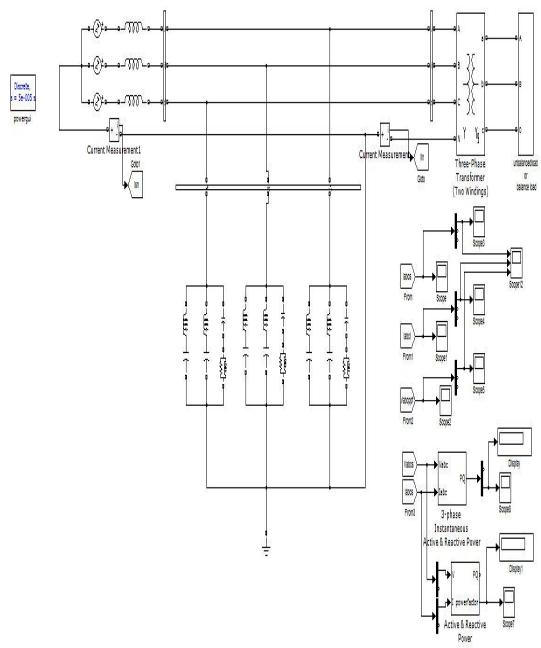

Figure 11: Wave form of Balanced Load for PPF-Conventional Method

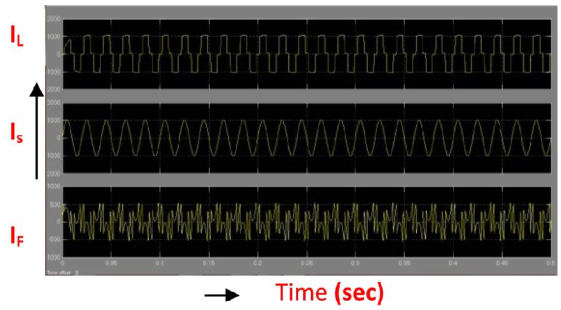

Figure 12: Wave Form of Unbalanced Load for PPF-Conventional Method

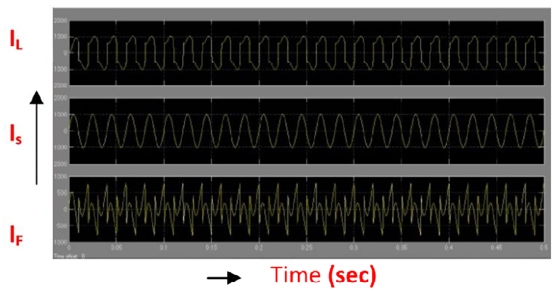

Figure 13: Wave Form of Balanced Load for PPF-PSO Method

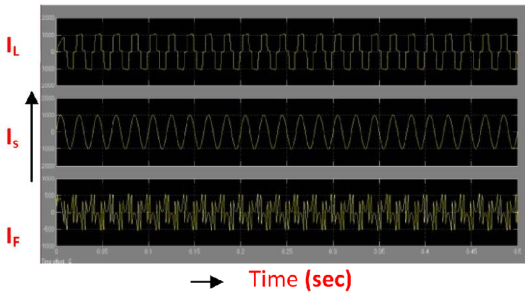

Figure 14: Wave Form of Unbalanced Load for PPF-PSO Method

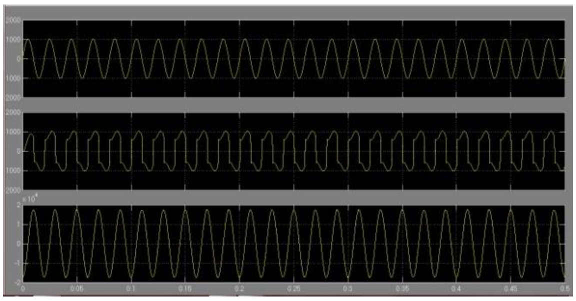

Table 7: Balance Load

Scheme	With PSO			Without PSO		
	% THD	PF	Reactive Power (VAR)	% THD	PF	Reactive Power (VAR)
PPF	1.53	0.936	1.172	26.54	0.5999	2.887

Table 7: Unbalance Load

Scheme	With PSO			Without PSO		
	% THD	PF	Reactive Power (VAR)	% THD	PF	Reactive Power (VAR)
PPF	1.53	0.940	1.103	33.68	0.7645	-8.025

CONCLUSION

A novel hybrid APF with injection circuit was proposed. Its principle and control methods were discussed. The proposed adaptive fuzzy-dividing frequency control can decrease the tracking error and increase dynamic response and robustness. The control method is also useful and applicable to any other active filters. It is implemented in an IHAPF with a 100-kVA APF system in a copper mill in Northern China, and demonstrates good performance for harmonic elimination. Simulation and application results proved the feasibility and validity of the IHAPF and the proposed control method.

REFERENCES

1. Bhattachaya S, Cheng P-T, Deep and Divan M (1997), "Hybrid Solutions for Improving Passive Filter Performance in High Power Applications", *IEEE Trans Ind. Appl.*, Vol. 33, No. 3, pp. 732-747.
2. Fujita H and Agaki H (1998), "The Unified Power Quality Conditioner: The Integration of Series and Shunt-Active Filters", *IEEE Trans. Power Electron.*, Vol. 13, No. 2, pp. 315-322.
3. Fujita H and Akagi H (1991), "A Practical Approach to Harmonic Compensation in Power System-Series Connection of Passive and Active Filters", *IEEE Trans. Ind. Appl.*, Vol. 27, No. 6, pp. 1020-1025.
4. Fukuda S and Imamura R (2005), "Application of a Sinusoidal Internal Model to Current Control of Three-Phase Utility-Interface Converters", *IEEE Trans. Ind. Electron.*, Vol. 52, No. 2, pp. 420-426.
5. Gyugyi L and Strycula E C (1976), "Active AC Power filters", in *Proc. IEEE, Ind. Appl. Soc. Annu. Meeting*, pp. 529-535.
6. Kim S and Enjeti P N (2002), "A New Hybrid Active Power Filter (APF)

Topology," *IEEE Trans. Power Electronics*, Vol. 17, No. 1, pp. 48-54.

7. Macken K J P, De Brabandere K M H A, Dnesen I J L and Belmans R J M (2001), "Evaluation of Control Algorithms for Shunt Active Tillers Under Unbalanced and Nonsinusoidal Conditions", in *Proc. IEEE Porta Power Tech. Conf., Porto*, September 10-13, pp. 1621-1626, Portugal.

8. Madtharad C and Premrudeepreechacharn S (2002), "Active Power Filter for Three-Phase Four-wire Electric Systems Using Neural Networks", *Elect. Power Syst. Res.*, Vol. 60, No. 2, pp. 179-192.

9. Malesani L, P. Mattavelli, and P. Tomasin, "High performance hysteresis modulation technique for active filters," IEEE Trans. Power Electron., vol. 12, no. 5, pp. 876–884, Sep. 1997.

10. Marks J H and Green T C (2002), "Predictive Transient-following Control of Shunt and Series Active Power Filters", *IEEE Trans. Power Electron.*, Vol. 17, No. 4, pp. 574-584.

11. Mohan N, Peterson H A, Long W F, Dreifuerst G R and Vithayathil J J (1977), "Active Filters for AC Harmonic Suppression," Presented at the *IEEE Power Eng. Soc. Winter Meeting*.

12. Nakajima A, Oku K, Nishidai J, Shiraishi T, Ogihara Y, Mizuki K and Kumazawa M (1988), "Development of Active Filter With Series Resonant Circuit", in *Proc 19th IEEE Annu. Power Electronics Specialists Conf. Rec.*, Vol. 2, April 11–14, pp. 1168-1173.

13. Nishida K, Konishi Y and Nakaoka M (2002), "Current Control Implementation With Deadbeat Algorithm for Three-Phase Current-Source Active Power Filter", *Proc. Inst. Elect. Eng., Electr. Power Appl.*, Vol. 149, No. 4, pp. 275-282.

14. Peng F, Akagi H and Nabae A (1990), "A New Approach to Harmonic Compensation in Power System: A Combined System of Shunt Passive and Series Active Filters", *IEEE Trans. Ind. Appl.*, Vol. 26, No. 6, pp. 983-990.

15. Ruixiang F, An L and Xinran L (2006), "Parameter Design and Application Research of Shunt Hybrid Active Power Filter", *Proc. CSEE*, Vol. 26, No. 2, pp. 106-111.

16. Yuan X, Merk W, Stemmler H and Allmeling J (2002), "Stationary-Frame Generalized Integrators for Current Control of Active Power Filters With Zero Steady-state Error For Current Harmonics of Concern Under Unbalanced and Distorted Operating Conditions", *IEEE Trans. Ind. Appl.*, Vol. 38, No. 2, pp. 523-532.